ISSN: 2641-192X
DOI: 10.33552/JTSFT.2023.10.000731
Journal of
Textile Science & Fashion Technology
Iris Publishers

Research Article

Microstructure-Crystallization Correlation with Surface Migration of Additives in High-Crystallinity Polypropylene Composites

Ji Eun Lee[1], Jong Sung Won[1], Eun Hye Kang[2], Hyeong Yeol Choi[3] and Seung Goo Lee[2]*

[1]*Defense Materials & Energy Technology Center, Agency for Defense Development, Daejeon 34060, Republic of Korea*

[2]*Department of Applied Organic Materials Engineering, Chungnam National University, Daejeon 34134, Republic of Korea*

[3]*Department of Fashion Design, Dong-A University, Busan 49315, Republic of Korea*

***Corresponding author:** Seung Goo Lee, Department of Applied Organic Materials Engineering, Chungnam National University, Daejeon 34134, Republic of Korea.

Received Date: April 07, 2023

Published Date: April 18, 2023

Abstract

This study aims to describe the crystallization structure and surface migration in polypropylene (PP) composites containing lubricants and talc during 0-72 h at 70 ℃ of accelerated thermal aging. The particles exposed on the surfaces of PP composites after accelerated aging are caused by lubricant components and certain types of talc migrating to the surface. This additive-migration phenomenon is found to be correlated to the surface migration of additives with the occurrence of secondary crystallization in PP composites owing to accelerated aging, which increases the heat of fusion, crystallinity, and nanocrystalline size. The accelerated aging evaluation method for PP composites adopted in this study reveals that the microstructure, crystallinity, crystal size, and heat of fusion are correlated. The findings of this study can be applied for improving the appearance and quality of composite products.

Keywords: Additive; Polypropylene; Composites; Migration; Slip agent

Introduction

Polymers can be found in almost all materials used in modern life, from everyday packaging to clothing, building, transportation, and communication, making it more convenient. One of the extensively used plastics is polypropylene (PP), which is expected to have other applications in future. However, PP is seldom used in its pure form, and its properties need to be improved for various applications [1-5]. With appropriate additives, its properties can be improved to render it particularly interesting in the field of thermoplastic materials. Lubricants are commonly used as additives in PP compounds because they include several advantages such as lubrication, release, and slip characteristics. Strong shear stresses are applied during compounding, under which the lubricant impregnates the compounds to reduce the viscosity and heat [6-8]. In addition, it functions as a release film and reduces the extrusion load on metal surfaces. The most common mineral additives in polymer compounds are mica, silica, and wollastonite, which are present in a range of 10 to 40% by weight. Among its numerous advantages, talc, a naturally hydrated magnesium silicate, has a wide variety of applications. As an additive, talc is particularly useful in polymeric matrices since it enhances rigidity, improves thermal properties, creates a nucleating effect, reduces shrinkage, and imparts dimensional stability. Talc has thus been widely used to compound materials for final automotive components, such as interior and exterior components of automobiles [9-14].

However, when a polymer plastic is exposed to the environment, the lubricants may migrate to the surface during the process or use, which may affect the health of consumers and deteriorate the product quality. In addition, plastic lubricants reduce the scission and crosslinking of macromolecular chains caused by thermooxidative factors. Untreated monomers and oligomers may also migrate to the surface of the plastic. The effectiveness of lubricants depends not only on their chemical structure but also on their physical parameters [15,16]. Several researchers have reported the migration of additives from polymer blends to the surfaces of plastic products. Moreover, toxicological studies on the genotoxicity of polymer additives have been published. Therefore, the determination of the additive content in polymers is a crucial component in the safety assessment of plastic packaging materials and plastic products, and quantification of the specific migration levels of these additives is also critical for the quality control of polymer plastics [17,18].

The additives to PP composites migrate to the surface, affecting the appearance of the product and deteriorating its physical properties. This study mainly focuses on the identification, classification, and suitability of additives that directly affect the quality and performance of the end-use products. Moreover, it describes the relationship between PP and the additive, depending on the product usage environment. A particular additive may comprise several components [19-21]. Therefore, it is important to under-stand the composition and purity of the additive, which is necessary for understanding the characteristics and correlation between each PP and additive. The development of analytical methods for the detection of these additives is critical. In particular, in the manufacture of high-quality polymer plastic products, a method for evaluating the correlation between polymers and additives is necessary to control the specific migration limits of additives with adverse toxicological properties. Analysis of all the mass-transport processes in the real migration of additives is highly complex because it involves the transport, permeation, or possible retention by environmental conditions of numerous components, as well as other compounds, which, if not transferred, may affect these processes [22,23]. Therefore, the system has been simplified, and each transferable compound analyzed separately. Moreover, environmental conditions have been assumed to be constant, and in many cases, accelerated assay conditions have been used (higher temperatures for shorter durations). Recent studies on global and specific migration (following international regulations, in many cases) have proven that the migration values are affected by long-term exposure to the environment [24-26]. In order to improve the understanding of the migration process at a molecular level, it is crucial to trace the migration process and quantify the migrating components in real polymer systems. Nevertheless, certain discrepancies arise when related studies are compared, and there is some uncertainty about the effects of diverse variables on migration, such as temperature, time, and additive composition [27-30].

With accelerated thermal aging of plastics, additives migrate to the specimen surfaces, which can cause problems in automotive applications. However, the blooming process of additives has not been described in detail in previous studies. Therefore, it is necessary to investigate the migration behavior of polymer additives and analyze the research results. We previously demonstrated that slip agents rapidly migrate to the surface by thermal aging, degrading the appearance quality and scratch resistance of PP composites [31]. In this study, we focus on the relationship between the crystalline behavior and temperature, and the migration of additives from the internal amorphous regions to the external surface of the specimen. We examine several test methods for confirming the migration behavior of additives in semi crystalline polymers subjected to an initial quality study and a durability quality study with thermal aging.

Materials and Methods

Materials and sample preparation

In this study, a high crystal PP block copolymer (JSS-350N, LOTTE Chemical, Re-public of Korea) with a melt flow rate of 10g/10min, rubber such as ethylene-octane copolymer elastomer (Engage8842, Dupont Dow Elastomer, USA) with a melt flow rate of 1.0 g/10 min and density of 0.86 g/cm^3, talc (IMIFABI) with an average particle size 0.5 μm, and two types of lubricants, magnesium stearate (Mg-st) and calcium stearate (Ca-st), with a molar mass of 500 g/mol (SD Korea, Republic of Korea) were used as received.

The composition of the PP compounds prepared in this study is listed in Table 1. To determine the additive migration mechanism, the composition ratio of stearic acid alone, mainly used in the automotive industry, was considered in this study for accurate measurement.

Table 1: Composition of the PP compounds prepared in this study Composition (wt%).

Composition (wt%)							
Composites	PP	Rubber (EOR)	Talc	Color- master batch	Stearic acid (Mg-st)	Stearic acid(Ca-st)	Aging time (h)
PP0/Mg	72.5	5	20	2	0.5	-	0
PP24/Mg	72.5	5	20	2	0.5	-	24
PP48/Mg	72.5	5	20	2	0.5	-	48
PP72/Mg	72.5	5	20	2	0.5	-	72
PP0/Ca	72.5	5	20	2	-	0.5	0
PP24/Ca	72.5	5	20	2	-	0.5	24
PP48/Ca	72.5	5	20	2	-	0.5	48
PP72/Ca	72.5	5	20	2	-	0.5	72

Under annealing conditions, we prepared three-mm-thick injection-molded specimens to demonstrate how additives diffuse to surfaces over time. Samples were annealed at 70 °C for 0, 24, 48, and 72 hours. For examining additive migration, specimens sized 127 mm × 127 mm x 3.0 mm were manufactured and then split into 10 mm × 10 mm × 1.0 mm samples to confirm the characteristics of additive migration between the interior and exterior specimens after accelerated thermal aging. These experiments were performed under the assumption that the internal additives diffused outward under the annealing conditions. Thus, the difference between each surface of the specimen can be identified. As part of this investigation, surface X-ray diffraction (XRD) and differential scanning calorimetry (DSC), as well as energy dispersive X-ray spectroscopy (EDS), were conducted on internal and external specimens to better understand additive migration. Figure 1 illustrates the sample preparation sequence.

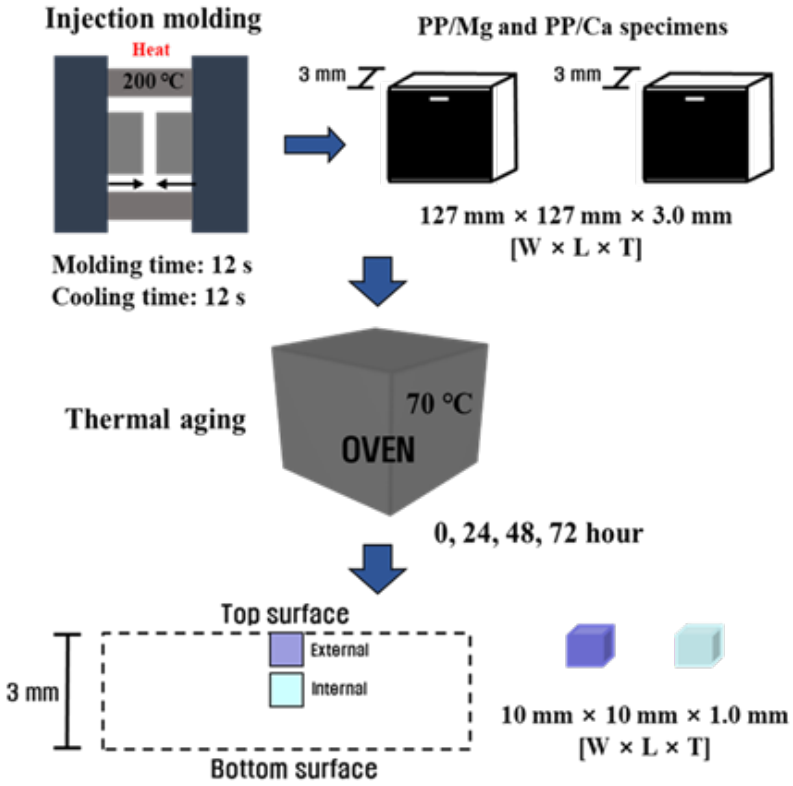

Figure 1: Illustration of the experimental procedure. Each specimen is annealed at 70 ˚C in an oven for 0, 24, 48, and 72 h. The specimens are cut in order to measure the internal and external crystallite sizes through XRD (Mg: magnesium stearate; Ca: calcium stearate; additives: rubber, talc, and color master batch).

Morphological analyses through SEM and EDS

The surface morphologies of the samples were determined and elemental analysis was performed using a digital camera (IFS-28, Canon) and a low-voltage field-emission scanning electron microscope (FE-SEM) equipped with an EDS. Elemental mapping analysis was performed to observe the changes in the morphology and elemental com-position under the annealing conditions.

X-ray diffraction analysis

Each XRD experiments were performed at room temperature using a Bruker AXS D8 system with a Cu-tube target (1.541 Å) in the standard continuous scan mode. The equipment was operated at 40 kV 40 mA. The scanning speed was 1.0 °/min, and the 2θ range was 5°-80°. Measurements were performed on 10×10×1.0 mm^3 internal and external samples. Based on the diffraction patterns measured through XRD analysis, the figures were obtained using Origin software. The Scherrer equation was used to calculate the crystallite size of the crystalline materials. The sizes of the particles in the crystals were calculated using the Scherrer equation [32,33]:

$$S = \frac{180}{\pi} \frac{K\lambda}{\cos\theta\sqrt{(FWHM)^2 - S^2}} \quad (1)$$

where λ is the wavelength (nm), K is a constant of a dimensionless shape factor, FWHM is the line broadening at half the maximum intensity per unit cell, 180/π converts the FWHM from degrees to radians, θ is the wavelength of the radiation (Å), and s is the broadening factor of the instrument.

Thermal analysis through DSC

The thermal characteristics of compound specimens were measured using Pyris-1 DSC (PerkinElmer). 5 mg specimens were heated to 25-200 °C at a rate of 10 °C/min and were maintained at 200 °C for 10 min and then cooled to 25 °C at the same rate under a nitrogen atmosphere throughout all tests.

Based on the quantification of the heat associated with polymer melting, the DSC was used to determine the degree of crystallinity of the polymer materials. The thermal history of the melt affects the crystallization behavior of polymers. Crystallization can be assessed by measuring the area under the endotherm from the start of melting to the end of crystallization. The degree of crystallinity was calculated as [34]:

$$X_c = \frac{\Delta H_m}{\Delta H_{100\%}} \quad (2)$$

where ΔH_m is the measured melting enthalpy of the samples and $\Delta H_{100\%}$ is the melting enthalpy of 100% crystalline PP, which is approximately 207 J/g [35].

Results and Discussion

Migration morphology

The accelerated thermal aging causes the additives to migrate to the specimen surface, resulting in "blooming" and "whitening". We examined the morphological properties of PP composites using a digital camera and SEM-EDS before and after thermal aging. Figure 2 displays images of morphological changes in PP/Ca and PP/Mg compo-sites caused by thermal aging of various durations. A large amount of lubricant migration to the surface is observed in PP/Mg composites aged for 0–72 h (Figures 2(a1-a4)). Lubricant migration is considerably slower in PP/Ca composites aged for 48 h com-pared to PP/Mg composites. This result indicates that the PP/Mg composite exhibits faster migration after aging from 0-72 h compared to the PP/Ca composite. These changes were confirmed through surface elemental analysis. The EDS results showing the migration of additives are presented in Figures 3 and 4. In Figures 3a and 4a, PP0/Mg and PP0/Ca do not exhibit significant lubricant migration, whereas migration of the lubricant onto the sample surface can be observed in PP/Mg and PP/Ca composites thermally aged for 24, 48, and 72 h (Figures 3(b-d) and Figures 4(b-d)). This is evidenced by the elemental composition of the samples under each condition (Table 2). Elemental mapping analysis shows that lubricant migration on the surface of the sample annealed for 72 h (samples shown in Figures 3d and 4d) is accelerated due to thermal aging com-pared to the unannealed sample (samples shown in Figures 3a and 4a).

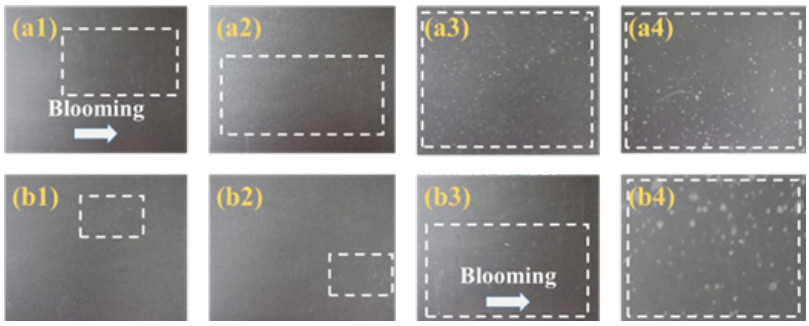

Figure 2: Close-up distal images of (a) PP/Mg composites and (b) PP/Ca composites aged at 70 °C for different time durations ((a1, b1): 0 h; (a2, b2): 24 h; (a3, b3): 48 h; (a4, b4) 72 h).

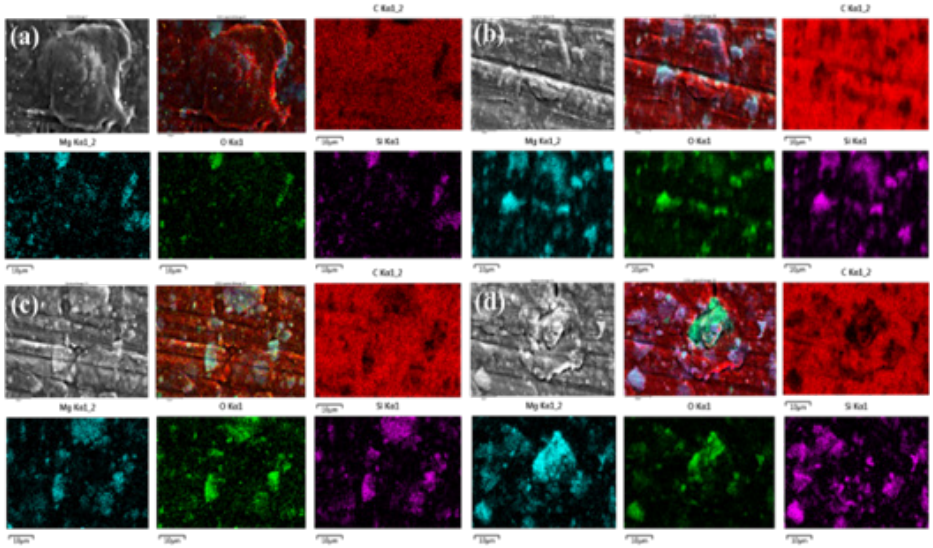

Figure 3: FESEM/EDS mapping showing the distribution of carbon (C), oxygen (O), magnesium (Mg), and silicon (Si) on PP/Mg composites aged at 70 °C for different time durations: (a) 0 h, (b) 24 h, (c) 48 h, and (d) 72 h.

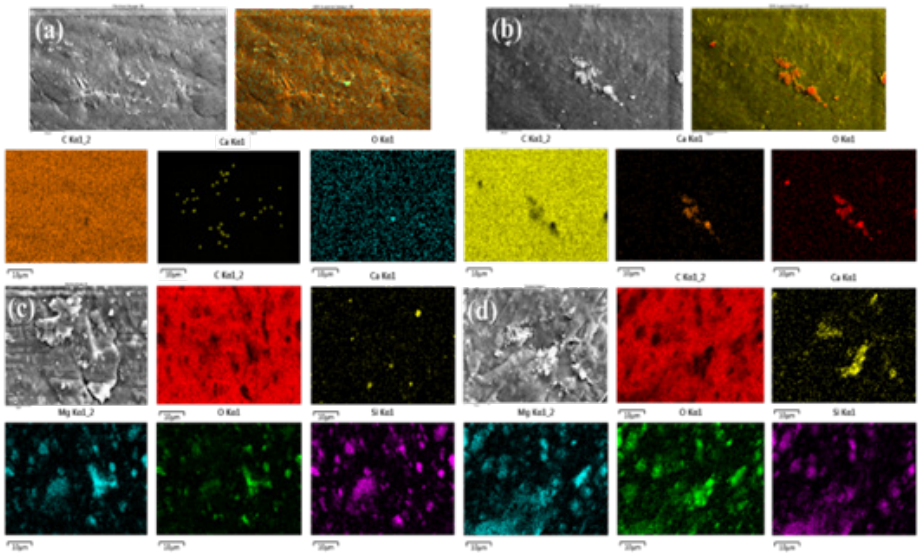

Figure 4: FESEM/EDS mapping showing the distribution of carbon (C), oxygen (O), calcium (Ca), magnesium (Mg), and silicon (Si) on PP/Ca composites aged at 70 °C for different durations: (a) 0, (b) 24, (c) 48, and (d) 72 h.

Table 2 shows the elemental compositions of the sample surfaces under different conditions, determined through EDS analysis. PP72/Mg and PP72/Ca (Figures 3d and 4d) have relatively large quantities of Mg, Ca, and Si atoms compared to PP0/Mg and PP0/Ca (Figures 3a and 4a). These higher elemental contents are attributed to the constitutive units of stearic acid containing Mg, Ca, and talc (natural hydrated magnesium silicate). The elemental mapping images of the samples displayed in Figures 3 and 4 show the elemental distribution on the composite surfaces. The presence of Mg and Si in the samples suggest that talc migration occurs during thermal aging. Therefore, as shown in Figure 5, accelerated thermal aging contributes to the increase in the elemental contents of the samples, which show a linearly proportional tendency.

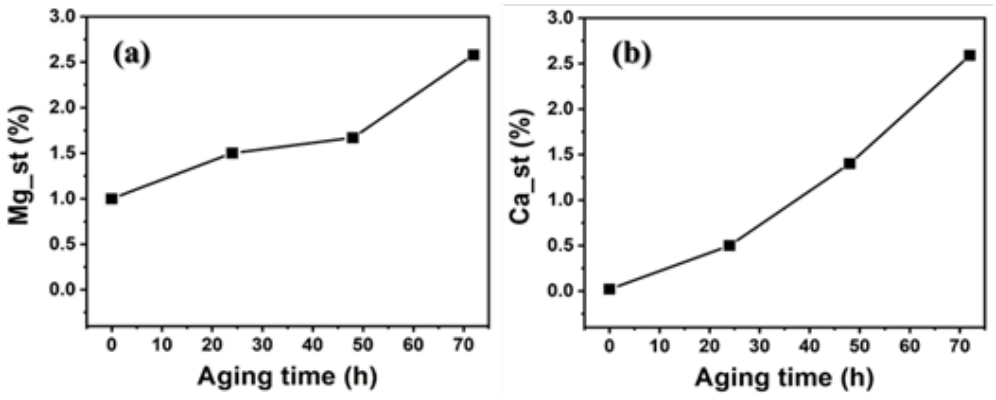

Figure 5: Relationship between the elemental composition and aging time of (a) PP/Mg composites; (b) PP/Ca composites aged at 70 °C for different durations (0–72 h).

Table 2: Elemental composition of the samples measured through EDS.

Sample	C (wt%)	O (wt%)	Mg (wt%)	Si (wt%)	
PP0/Mg	91.45	6.16	1	1.39	
PP24/Mg	88.1	8.31	1.53	2.02	
PP48/Mg	87.03	8.66	1.83	2.47	
PP72/Mg	85.36	9.85	2.58	2.21	
Sample	C (wt%)	O (wt%)	Ca (wt%)	Mg (wt%)	Si (wt%)
PP0/Ca	97.68	2.3	0.02	0	0

PP24/Ca	97.22	2.72	0.5	0	0
PP48/Ca	86.9	8.09	1.4	1.62	1.99
PP72/Ca	86.78	8.22	2.59	1.51	1.7

Crystal structure of PP compounds

We Accelerated aging experiments involving annealing of the external and internal sample surfaces were performed at 70 °C for 0, 24, 48, and 72 h. While there are almost no differences in the crystal structures of the external and internal regions, additive migration to each sample surface is observed at different thermal aging durations. The XRD profiles depicted in Figures 6 and 7 exhibit the changes in the intensity of the crystal-line structures of the external and internal PP/lubricant composites thermally aged at 70 °C for 0, 24, 48, and 72 h. XRD analysis cannot quantitatively measure the amount of additive migration. It is qualitatively confirmed that the intensity of the talc peaks is proportional to the amount of migrated lubricant for 0, 24, 48, and 72 h of thermal aging. As shown in Figures 6 and 7, the internal talc migrates to the surfaces of the compo-sites on annealing, increasing the intensity of the external peaks of the talc (T) (001), (002), (003), and (020). In addition, the results show mass concentrations of the phases of the additive components on the composite surface. Thus, these results indicate that migration occurs because of the effect of annealing.

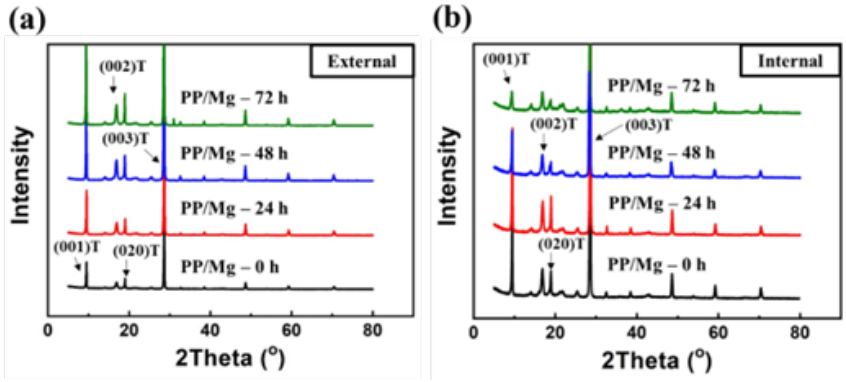

Figure 6: X-ray diffraction profiles of external and internal PP/Mg composites containing additives, for 0, 24, 48, and 72 h of thermal aging at 70 ˚C.

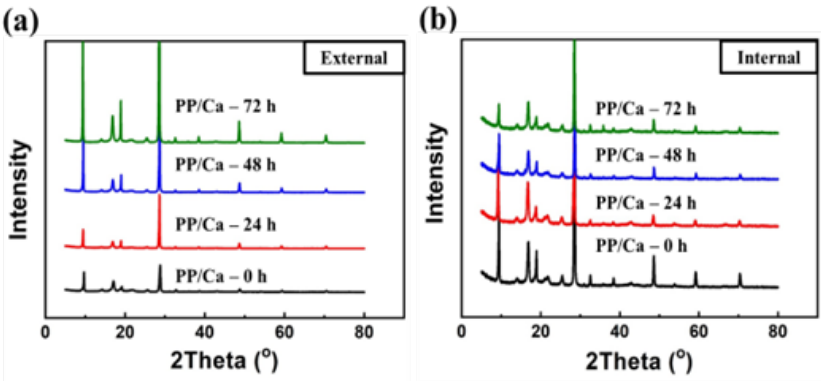

Figure 7: X-ray diffraction profiles of external and internal PP/Ca composites containing additives, for 0, 24, 48, and 72 h of thermal aging at 70 ˚C.

Crystallite size

As a result of thermal aging, the additive migration and crystallite size correlations are confirmed. XRD measurements indicate a correlation between accelerated aging time and spheroid size (nm). The crystallinity may eventually be larger than its initial size due to thermal aging below melting temperature. As a result, low-molecular-weight lubricant additives migrate to the composite surface; these additives are particularly concentrated in the mobile amorphous regions of the PP. Thermal aging, however, changes the amorphous fraction and entangles the molecular chains in the migratory domains, resulting in limited motion, such as secondary crystallization, during thermal aging. Therefore, because of the entanglement of the intracrystalline chains, the lamellae thicken, and the crystallite size increases with the increase in the thermal aging

duration. Hence, as shown in Figure 8, the crystallite size increases with thermal aging from 0-72 h. The compound melts have different crystallite sizes on the external and internal surfaces owing to thermal hysteresis during injection molding.

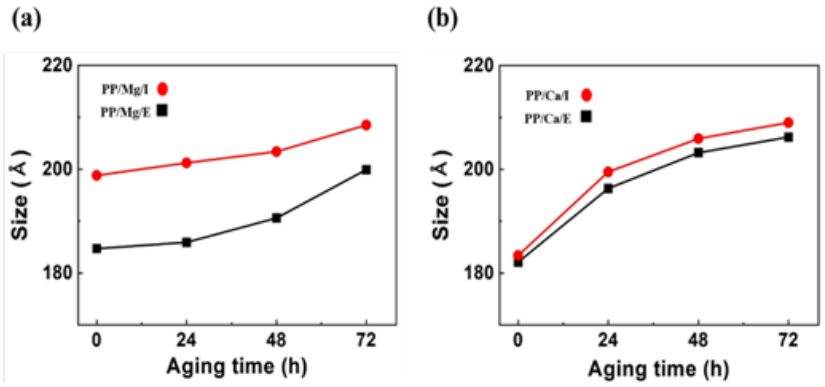

Figure 8: Crystallite sizes of the samples determined thorough XRD analysis at different annealing periods, as described in Table 3 (■: External (E) surface; ●: Internal (I) surface).

The PP crystal size is influenced by the type of nucleating agent, thermal hysteresis, and temperature. Fast nucleation and small crystal grains are formed as a result of rapid quenching. After the initial nucleus is formed, the crystal size can change again due to thermal aging. As a result of this study, we confirm that the crystallite size increases under accelerated aging and that the additives in amorphous regions diffuse to the surface. Thus, the increase in crystallization size is responsible for the migration of lubricant from PP to the surface. The FWHM and crystallite sizes are listed in Table 3. Nevertheless, it should be noted that this calculation only takes XRD parameters into account. Because talc is inorganic, it exhibits a higher intensity peak than PP in the XRD analysis. Therefore, it is necessary to distinguish between the peaks of PP and talc.

Table 3: Comparison of the peak widths and crystallite sizes of the external (E) and internal (I) surfaces of PP/Mg and PP/Ca compounds.

Sample	2θ (°)	FWHM(deg)	Crystallite Size (nm)	Sample	2θ (°)	FWHM(deg)	Crystallite Size (nm)
PP0/Mg/E	16.9099	0.4512	185.9	PP0/Mg/I	16.0445	0.4165	201.2
PP24/Mg/E	16.9276	0.4541	184.7	PP24/Mg/I	15.783	0.411	198.8
PP48/Mg/E	16.8566	0.4401	190.6	PP48/Mg/I	15.428	0.401	203.4
PP72/Mg/E	16.8592	0.4196	199.9	PP72/Mg/I	15.369	0.391	208.5
PP0/Ca/E	15.428	0.448	182.1	PP0/Ca/I	16.8816	0.4574	183.4
PP24/Ca/E	15.645	0.416	196.3	PP24/Ca/I	16.857	0.409	189.5
PP48/Ca/E	15.704	0.402	203.2	PP48/Ca/I	16.857	0.411	199.9
PP72/Ca/E	15.625	0.396	206.2	PP72/Ca/I	16.808	0.393	209

The SEM and EDS analysis of PP/lubricant composites with less additive migration (Figures 3a and 4a) with those of PP/lubricant composites with more additive migration (Figures 3d and 4d) show that thermal aging conditions accelerate the increase in crystallite size and migration of the lubricants in PP, thus reducing the amorphous regions. Amorphous lubricant migrates to the surface of the composite over time, indicating that the lubricant is present there. Figure 9 shows a linear relationship, and these results suggest that the size of crystallites affects the amount of additives.

Heat of Fusion

Figure 10 shows the DSC thermograms for different thermal aging durations for the external and internal samples. The melting endotherms of the composites show changes due to the crystallization increase caused by thermal aging.

As previously described (Figure 8), due to the thin lamellar stacks formed by the crystallization of the remaining mobile lamellae between the primary stacks, the average size of the crystals increases with thermal aging for 0, 24, 48, and 72h. Studies on crystallinity suggest that rearrangements, such as secondary crystallization of semi-crystalline polymers, may be associated with changes in the crystalline and amorphous regions of PP with thermal aging [36,37]. Due to the entanglement of the lamellar stack in the intercrystalline region, the lamellar stack in the amorphous region exhibits a certain degree of mobility. The result shows that the PP heat of fusion increases slightly under various thermal aging conditions, as shown in Figure 8, which is considered evidence of secondary crystallization in the thicker crystals. The increase in heat of fusion is an indication of crystallinity in the sample. In Figure 11, the heat of fusion is linearly related to the crystallite size of samples thermally aged for 0, 24, 48, and 72 hours.

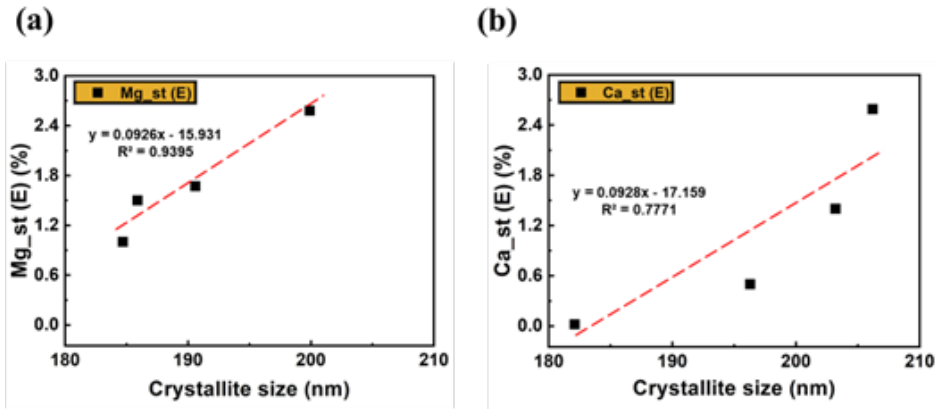

Figure 9: Relationship between the elemental composition of the additives and crystallite size for 0, 24, 48, and 72 h of thermal aging.

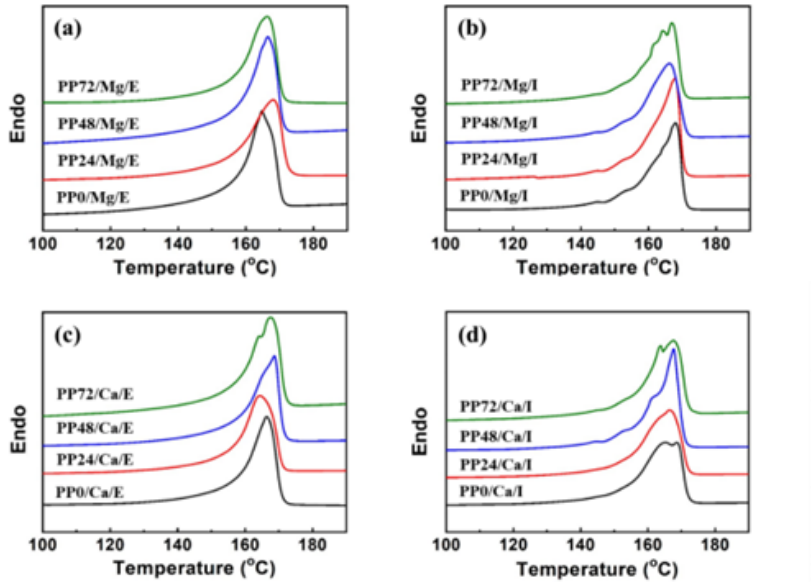

Figure 10: DSC thermograms of external and internal PP/Mg and PP/Ca samples annealed at 70 ˚C for 0, 24, 48, and 72 h.

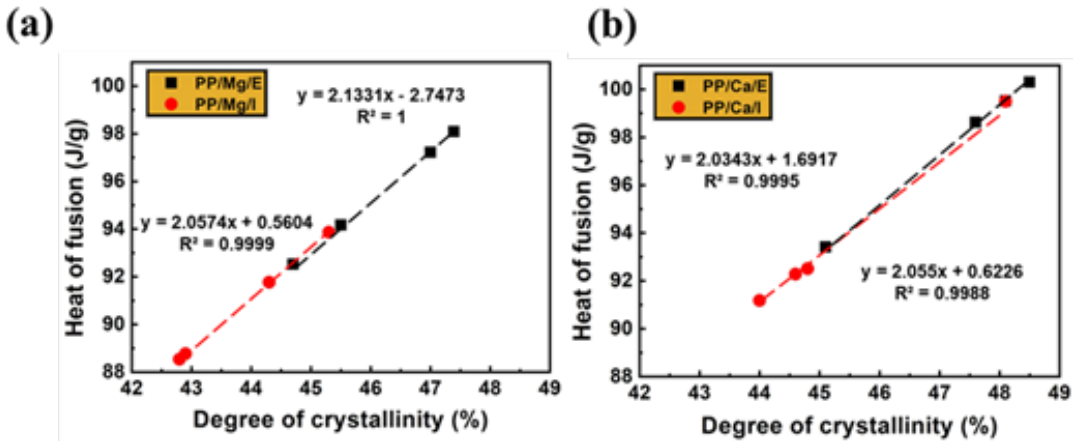

Figure 11: Relationship between the heat of fusion (J/g) and crystallite size (nm) of samples thermally aged for 0, 24, 48, and 72 h.

Table 4 presents the DSC results, including the melting peak (T_m), crystallization peak (T_c), heat of fusion (ΔH_m), and degree of crystallinity (X_c). The crystallization value can be analyzed by integrating the region under the endotherm and dividing it by the heat of fusion of 100% crystalline PP (Equation 2).

Table 4: DSC data of samples annealed at 70 ˚C for different durations.

Composite	T_m (˚C)		T_c (˚C)		ΔH_m (J/g)		Degree of crystallinity (%)	
	E	I	E	I	E	I	E	I
PP0/Mg	164.7	167.8	128.2	128.5	92.529	88.535	44.7	42.8
PP24/Mg	168.1	167.6	128.1	128.5	94.171	88.771	45.5	42.9
PP48/Mg	166.2	166	128.5	127.9	97.224	91.767	47	44.3
PP72/Mg	166.3	166.8	128.1	128.3	98.093	93.871	47.39	45.3
PP0/Ca	166.1	165	128.3	127.9	93.416	91.18	45.1	44
PP24/Ca	164.3	166.1	128.3	128.5	98.629	92.285	47.6	44.6
PP48/Ca	168.4	167.4	127.9	128.4	99.519	92.506	48.1	44.8
PP72/Ca	167.4	167.4	128.3	128.2	100.303	99.502	48.5	48.1

Due to the increased crystallinity of crystalline and amorphous regions by accelerated aging, the heat of fusion and crystallinity are slightly increased. This result suggests that the increase in the melting enthalpy is related to the increase in the crystallite size and decrease in the amorphous region. It is proved that the additive located in the amorphous region moves to the surface because of thermally accelerated aging and solidifies, not only deteriorating the final product but also reducing the function of the additive.

Conclusions

The main purpose of our study was to examine the propensity for surface migration of lubricant additives during accelerated thermal aging and determine whether this propensity could be described in terms of the crystallite size and microstructure. The SEM and EDS results of samples annealed at 70 ℃ for 0-72h revealed the presence of additives on the sample surfaces, particularly Mg-st, Ca-st, and talc. Composites aged for 72h exhibited significant blooming effects compared to those before accelerated aging, manifested as whitening on the sample surface. The blooming phenomenon on the sample surface was correlated with the XRD peak intensities of PP and talc of external samples thermally aged at 70 ℃ for 72h. With the increase in the XRD peak intensity of the external sample, the lubricant additives observed on the surface increased. Additionally, the average crystallite size was increased by the surface migration of additives due to thermal aging for 0-72 h. This indicates a linear relationship between the crystallite size and the degree of movement to the sample surface. Moreover, the increase in the heat of fusion is a direct indication of thicker lamellae and higher crystallinity. The higher heat of fusion forms secondary lamellae, and the degree of migration is proportional to the crystallite size and enthalpy of melting of the sample during thermal aging. Using the accelerated aging test method, this study reveals that the blooming phenomenon, which deteriorates the surface quality of PP/lubricant composites, is correlated to the microstructure and crystal structure.

Acknowledgement

This work was supported by research fund of Chungnam National University.

Conflict of Interest

The authors declared no potential conflicts of interest with respect to the research, authorship, and /or publication of this article.

References

1. Kawasumi M, Hasegawa N, Kato M, Usuki A, Okada A (1997) Preparation and Mechanical Properties of Polypropylene–Clay Hybrids. Macromolecules 30: 6333-6338.
2. Tordjeman Ph, Robert C, Marin G, Gerard P (2001) The Effect of α, β Crystalline Structure on the Mechanical Properties of Polypropylene. The European Physical Journal E 4: 459-465.
3. Khunova V, Zamorsky Z (1993) Studies on the Effect of Reactive Polypropylene on the Properties of Filled Polyolefin Composites. Part 1. Advantages of Solid-Phase-Grafted Maleated Polypropylene Over Melt-Phase-Modified Polymers. Polymer-Plastics Technology and Engineering 32(4): 289-298.
4. Shmueli Y, Lin YC, Lee S, Zhernenkov M, Tannenbaum R, et al. (2019) In Situ Time-Resolved X-Ray Scattering Study of Isotactic Polypropylene in Additive Manufacturing. ACS Appl Mater Interfaces 11(40): 37112-37120.
5. Jin M, Neuber C, Schmidt HW (2020) Tailoring Polypropylene for Extrusion-Based Additive Manufacturing. Additive Manufacturing 33: 101101.
6. Martín-Alfonso JE, Valencia C, Franco JM (2013) Effect of Amorphous/Recycled Polypropylene Ratio on Thermo-Mechanical Properties of Blends for Lubricant Applications. Polymer Testing 32(3): 516-524.
7. Hernández Y, Lozano T, Morales-Cepeda AB, Navarro-Pardo F, Ángeles ME, et al. (2019) Stearic Acid as Interface Modifier and Lubricant Agent of the System: Polypropylene/Calcium Carbonate Nanoparticles. Polymer Engineering & Science 59(s2): E279-E285.
8. Hristov V, Vlachopoulos J (2007) Thermoplastic Silicone Elastomer Lubricant in Extrusion of Polypropylene Wood Flour Composites. Advances in Polymer Technology 26(2): 100-108.

9. Uysal M, Tanyildizi H (2012) Estimation of Compressive Strength of Self Compacting Concrete Containing Polypropylene Fiber and Mineral Additives Exposed to High Temperature Using Artificial Neural Network. Construction and Building Materials 27(1): 404-414.

10. Zhou Y, Rangari V, Mahfuz H, Jeelani S, Mallick PK (2005) Experimental Study on Thermal and Mechanical Behavior of Polypropylene, Talc/Polypropylene and Polypropylene/Clay Nanocomposites. Materials Science and Engineering: A 402(1-2): 109-117.

11. Wang K, Bahlouli N, Addiego F, Ahzi S, Rémond Y, et al. (2013) Effect of Talc Content on the Degradation of Re-Extruded Polypropylene/Talc Composites. Polymer Degradation and Stability 98(7): 1275-1286.

12. Qiu F, Wang M, Hao Y, Guo S (2014) The Effect of Talc Orientation and Transcrystallization on Mechanical Properties and Thermal Stability of the Polypropylene/Talc Composites. Composites Part A: Applied Science and Manufacturing 58: 7-15.

13. Lapcik Jr L, Jindrova P, Lapcikova B, Tamblyn R, Greenwood R, et al. (2008) Effect of the Talc Filler Content on the Mechanical Properties of Polypropylene Composites. Journal of Applied Polymer Science 110(5): 2742-2747.

14. Shelesh-Nezhad K, Taghizadeh A (2007) Shrinkage Behavior and Mechanical Performances of Injection Molded Polypropylene/Talc Composites. Polymer Engineering & Science 47(12): 2124-2128.

15. Garde JA, Catalá R, Gavara R, Hernandez RJ (2001) Characterizing the Migration of Antioxidants from Polypropylene into Fatty Food Simulants. Food Addit Contam 18(8): 750-762.

16. Brostow W, Deshpande S, Fan K, Mahendrakar S, Pietkiewicz D, et al. (2009) Gamma-Irradiation Effects on Polypropylene-Based Composites with and without an Internal Lubricant. Polymer Engineering & Science 49(5): 1035-1041.

17. Wang Q, Storm BK (2006) Migration Study of Polypropylene (PP) Oil Blends in Food Simulants. Macromolecular Symposia 242(1): 307-314.

18. Xie M, Liu X, Li H (2006) Influence of Poly(Ethylene Glycol)-Containing Additives on Extrusion of Ultrahigh Molecular Weight Polyethylene/Polypropylene Blend. Journal of Applied Polymer Science 100(2): 1282-1288.

19. Spatafore R, Pearson LT (1991) Migration and Blooming of Stabilizing Antioxidants in Polypropylene. Polymer Engineering & Science 31(22): 1610-1617.

20. Nouman M, Saunier J, Jubeli E, Yagoubi N (2017) Additive Blooming in Polymer Materials: Consequences in the Pharmaceutical and Medical Field. Polymer Degradation and Stability 143: 239-252.

21. Dasari A, Misra RDK (2004) The Role of Micrometric Wollastonite Particles on Stress Whitening Behavior of Polypropylene Composites. Acta Materialia 52(6): 1683-1697.

22. Földes E (1998) Study of the Effects Influencing Additive Migration in Polymers. Die Angewandte Makromolekulare Chemie 261-262(1): 65-76.

23. Hinder SJ, Lowe C, Maxted JT, Watts JF (2005) Migration and Segregation Phenomena of a Silicone Additive in a Multilayer Organic Coating. Progress in Organic Coatings 54(2): 104-112.

24. Hou J, Zhao G, Wang G (2021) Polypropylene/Talc Foams with High Weight-Reduction and Improved Surface Quality Fabricated by Mold-Opening Microcellular Injection Molding. Journal of Materials Research and Technology 12: 74-86.

25. O'Brien A, Cooper L (2001) Polymer Additive Migration to Foods--a Direct Comparison of Experimental Data and Values Calculated from Migration Models for Polypropylene. Food Addit Contam 18(4): 343-355.

26. Brzozowska-Stanuch A, Rabiej S, Fabia J, Nowak J (2014) Changes in Thermal Properties of Isotactic Polypropylene with Different Additives during Aging Process (in English) 59: 302-307

27. Kirchkeszner C, Petrovics N, Tábi T, Magyar N, Kovács J, et al. (2022) Swelling as a Promoter of Migration of Plastic Additives in the Interaction of Fatty Food Simulants with Polylactic Acid- and Polypropylene-Based Plastics. Food Control 132: 108354.

28. Zhu S, Hirt DE (2007) Hydrophilization of Polypropylene Films by Using Migratory Additives. Journal of Vinyl and Additive Technology 13(2): 57-64.

29. Alberto Lopes J, Tsochatzis ED, Robouch P, Hoekstra E (2019) Influence of Pre-Heating of Food Contact Polypropylene Cups on Its Physical Structure and on the Migration of Additives. Food Packag Shelf Life 20: 100305.

30. Begley TH, Brandsch J, Limm W, Siebert H, Piringer O (2008) Diffusion Behaviour of Additives in Polypropylene in Correlation with Polymer Properties. Food Addit Contam Part A Chem Anal Control Expo Risk Assess 25(11): 1409-1415.

31. Won JS, Lee JM, Lee PG, Choi HY, Kwak TJ, et al. (2022) Effects of Nanocrystallization on Surface Migration of Polypropylene/Slip Agent Composites in Accelerated Aging. Journal of Materials Science 57: 1489-1505.

32. Benetti EM, Causin V, Marega C, Marigo A, Ferrara G, et al. (2005) Morphological and Structural Characterization of Polypropylene Based Nanocomposites. Polymer 46(19): 8275-8285.

33. Song F, Huang L, Chen D, Tang W (2008) Preparation and Characterization of Nanosized Zn–Co Spinel Oxide by Solid State Reaction Method. Materials Letters 62(3): 543-547.

34. Perrin-Sarazin F, Ton-That MT, Bureau MN, Denault J (2005) Micro- and Nano-Structure in Polypropylene/Clay Nanocomposites. Polymer 46(25): 11624-11634.

35. Bu HS, Cheng SZD (1988) Wunderlich B. Addendum to the Thermal Properties of Polypropylene. Die Makromolekulare Chemie, Rapid Communications 9: 75-77.

36. Li XM, Yang RJ (2006) Study on Blooming of Tetrabromobisphenol a Bis(2,3-Dibromopropyl Ether) in Blends with Polypropylene. Journal of Applied Polymer Science 101(1): 20-24.

37. Mezghani K, Anderson Campbell R, Phillips PJ (1994) Lamellar Thickening and the Equilibrium Melting Point of Polypropylene. Macromolecules 27: 997-1002.